Pergamon

Pattern Recognition, Vol. 29, No. 11, pp. 1775–1788, 1996

0031-3203/96 $15.00 + .00

PII: S0031-3203(96)00038-6

INTRINSIC PARAMETER CALIBRATION PROCEDURE FOR A (HIGH-DISTORTION) FISH-EYE LENS CAMERA WITH DISTORTION MODEL AND ACCURACY ESTIMATION*

SHISHIR SHAH and J. K. AGGARWAL

Computer and Vision Research Center, Department of Electrical and Computer Engineering, ENS 522, The University of Texas at Austin, Austin, TX 78712-1084, U.S.A.

(*Received* 8 *August* 1995; *in revised form* 12 *February* 1996; *received for publication* 28 *February* 1996)

Abstract—This paper presents a calibration procedure for a fish-eye lens (a high-distortion lens) mounted on a CCD TV camera. The method is designed to account for the differences in images acquired via a distortion-free lens camera setup and the images obtained by a fish-eye lens camera. The calibration procedure essentially defines a mapping between points in the world coordinate system and their corresponding point locations in the image plane. This step is important for applications in computer vision which involve quantitative measurements. The objective of this mapping is to estimate the internal parameters of the camera, including the effective focal length, one-pixel width on the image plane, image distortion center, and distortion coefficients. The number of parameters to be calibrated is reduced by using a calibration pattern with equally spaced dots and assuming a pin-hole model camera behavior for the image center, thus assuming negligible distortion at the image distortion center. Our method employs a non-linear transformation between points in the world coordinate system and their corresponding location on the image plane. A Lagrangian minimization method is used to determine the coefficients of the transformation. The validity and effectiveness of our calibration and distortion correction procedure are confirmed by application of this procedure on real images. Copyright © 1996 Pattern Recognition Society. Published by Elsevier Science Ltd.

Camera calibration Lens distortion Intrinsic camera parameters Fish-eye lens Optimization

1. INTRODUCTION

Accurate calibration of an imaging device is of utmost importance in computer vision. Precise camera calibration is needed in various applications which involve quantitative measurements, such as stereo vision, robot navigation, inspection and automated assembly, and robot vision. An important aspect of calibration is estimating the internal or intrinsic parameters of the camera. These parameters determine how the image coordinates of any point may be computed, given the three-dimensional (3-D) position of the point with respect to the camera. The estimation of the geometric relation between the camera and the scene is also an important aspect of the calibration procedure, and the parameters which characterize this relation are termed the external or extrinsic parameters. The estimation of extrinsic parameters has been well studied in the past and will not be detailed in this paper. On the other hand, researchers have neglected the estimation of intrinsic parameters, which in fact are crucial to a precise quantitative analysis.

Most cameras are not perfect and tend to show a variety of distortions and aberrations. For geometric measurements, the most important issue is the distortion that the camera exhibits. The cameras most commonly used have off-the-shelf lenses that exhibit a substantial amount of distortion. The camera assembly is often misaligned internally, and the CCD sensing array may not be orthogonal to the optical axis of the lens. Similar characteristics are inherent to the fish-eye lens camera, thus making it important to establish an efficient method of calibration before determining the camera distortion coefficients. The fish-eye lens proves to be useful where a large field of view is required, since it provides a field of view which is approximately 180°. When the distance between the lens and the object is small, a fish-eye lens can provide a full view of the object where other lenses fail to do so. To obtain accurate quantitative measurements from fish-eye lens images, we have to calibrate certain camera parameters so that we can accurately transform the image plane coordinates of the object into the 3-D world coordinates.

Although fish-eye lenses provide for a large field of view ($\sim 180°$), they introduce significant distortion in the image, as seen by comparing Figs 1 and 2.

* This research was supported in part by the DoD Joint Services Electronic Program through the Air Force Office of Scientific Research (AFSC) Contract F49620-92-C-0027, in part by the Army Research Office under contract DAAH-04-94-G-0417, and in part by the Texas Advanced Technology Program Grant ATP-442.

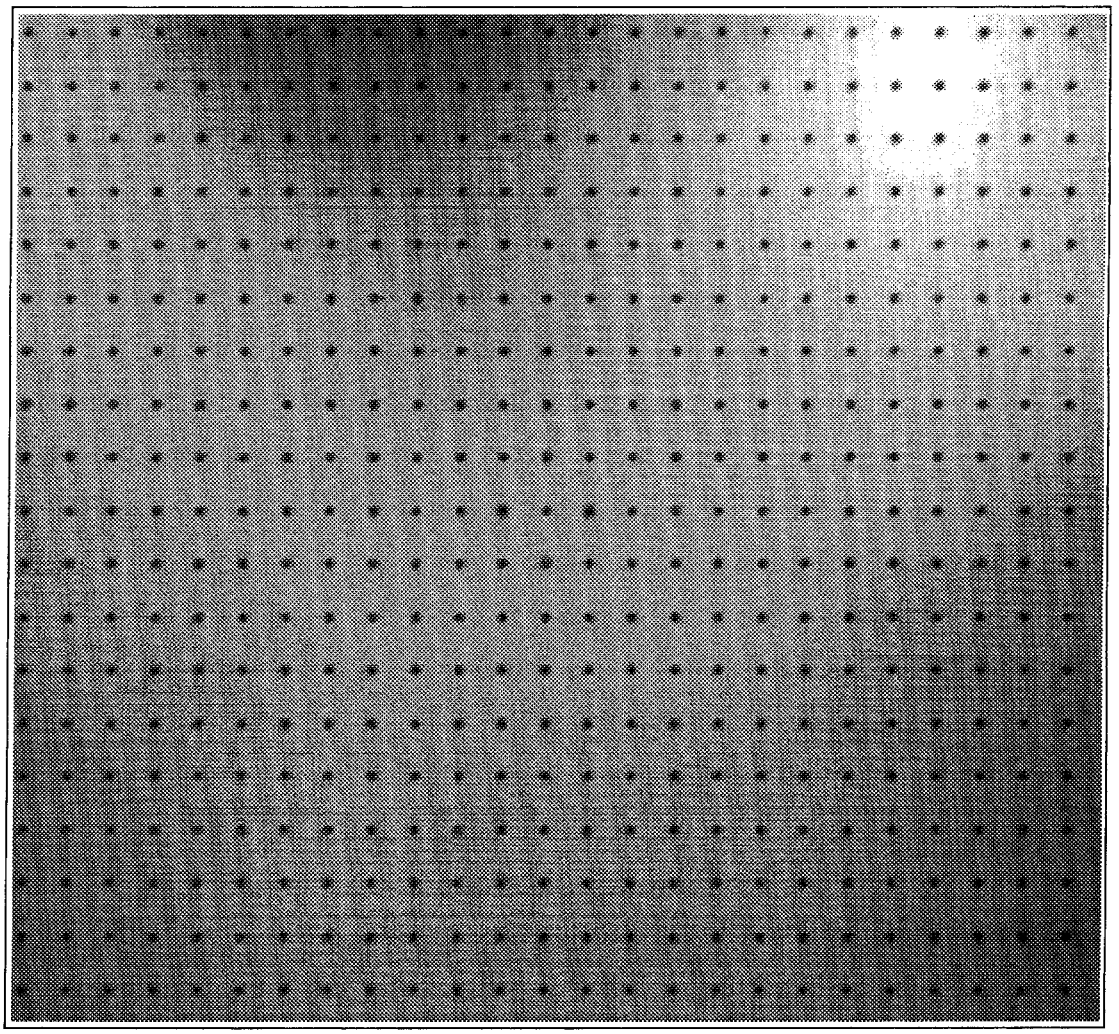

Fig. 1. The calibration pattern.

Figure 1 shows an image of the calibration pattern taken by a *normal* lens which introduces minimal distortion, while Fig. 2 shows an image of the same pattern taken by the fish-eye lens. The distortion results in a shifting of pixels from their orginal positions and the image tends to bend away from the optical center. The distortion seen is known as barrel distortion. Clearly, it is evident that correction of the image is important when using a fish-eye lens. In order to establish the camera model for the fish-eye lens camera, the intrinsic parameters must be determined and the distortion analysed. The parameters that need to be calibrated are:

(1) effective focal lengths,
(2) one-pixel width on the image plane,
(3) optical center,
(4) distortion coefficients.

This paper presents a simple and effective calibration method of intrinsic parameters for high distortion lens cameras.

This paper is organized into the following sections: Section 2 briefly reviews the previous work done in camera calibration, including the different distortion types involved. Section 3 describes the camera calibration method. The procedures for determining the optical center, the effective focal length, one-pixel width on the image plane, and evaluating the distortion coefficients employed for distortion correction are presented. The relation between the image plane points with their respective 3-D world coordinate points is also discussed. Section 4 presents the experimental results of the calibration procedure. Our method for testing the accuracy of the calibration procedure is described and its results are presented in Section 5. Finally, Section

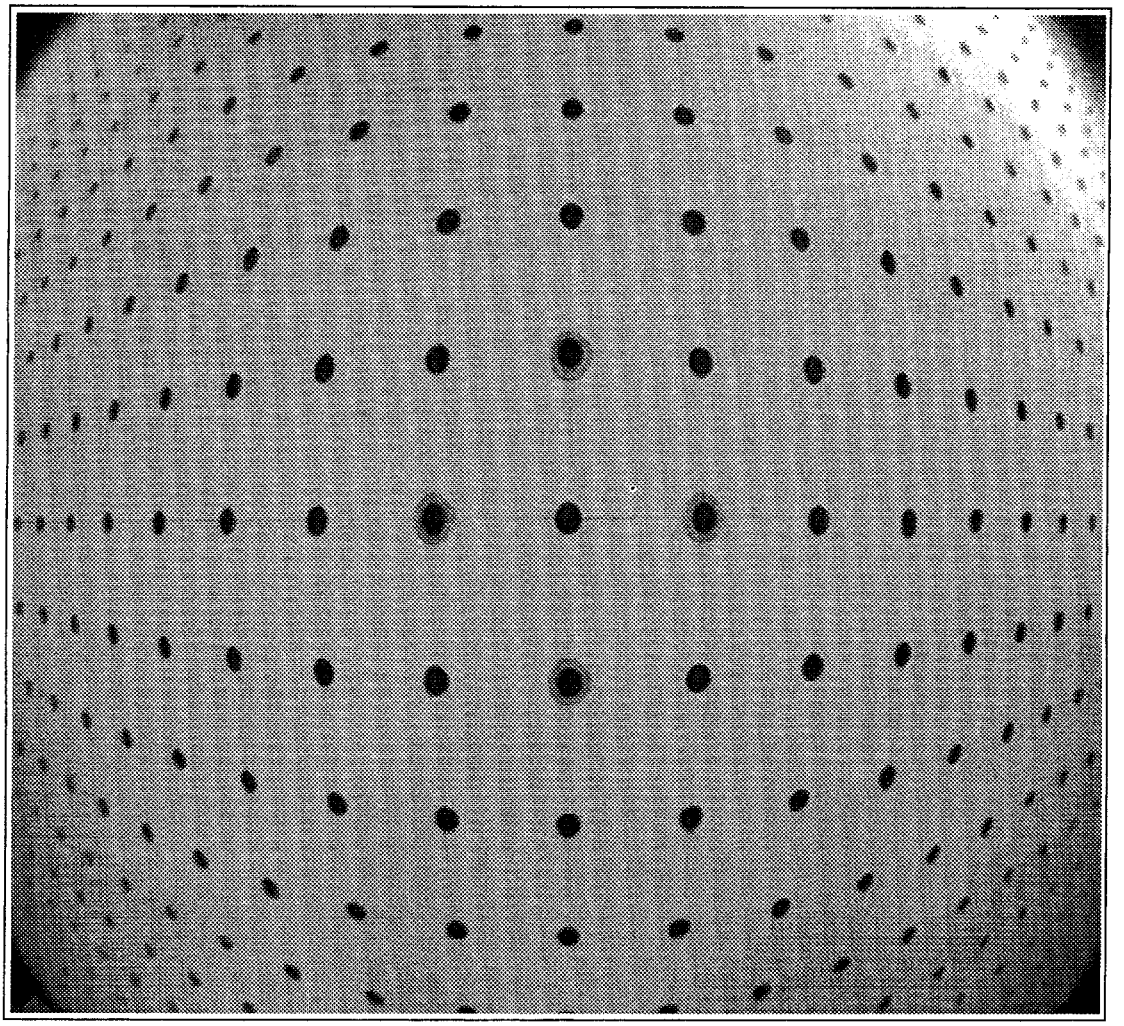

Fig. 2. Calibration pattern as imaged by fish-eye lens.

6 summarizes the calibration method, along with conclusions.

2. PREVIOUS WORK

In order to correct the inherent distortion of the fish-eye lens, it is important that each pixel in the distorted two-dimensional (2-D) image (x, y) be mapped to its original position from the 3-D scene (X, Y, Z) projected onto a 2-D plane (x', y') based upon the ideal pin-hole camera model. Each pixel in the image plane is shifted to a different position in the image due to the effects of distortion, which is mainly a result of the curvature of the lens.

Beck[1] and Miyamoto[2] describe several mapping methods which relate the angle in the world plane to a corresponding angle in the image plane. The angle in the world plane is the angle between the line that connects any point in the real world with the optical center and the optical axis, while its corresponding angle in the image plane is the angle between the line connecting the projection of that point in the image with the optical center and the optical axis. This is schematically shown in Fig. 3. The relation $2\tan(\phi'/2) = \tan(\phi)$ is used in the stereographic method, where ϕ' is the angle in the world plane and ϕ is the angle in the image plane. Using this mapping, a small circle in front of the camera always maps to a small circle in the image plane, but as the circle moves away from the center, the diameter in the image plane will change. In their equidistant projection method, the appropriate relation $\phi' = \tan(\phi)$ is used. In this mapping the small circle in the 3-D plane maps to an ellipse-like figure in the 2-D plane when the circle moves towards the edge and one of the diameters in the image plane stays constant. These methods correct the image near the optical center, but towards the image edge the distortion remains significant. Anderson, Alvertos and Hall[3] present a method in which the relationship between ϕ' and ϕ is established based on

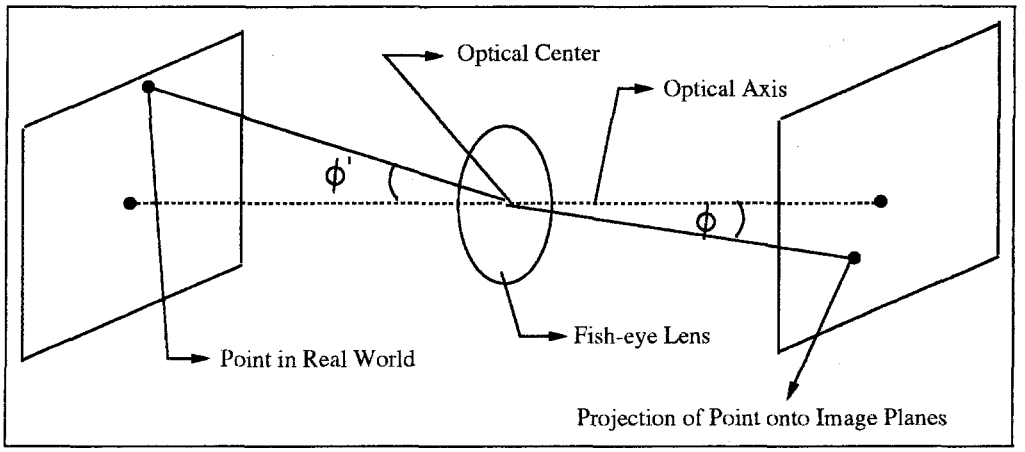

Fig. 3. World plane to image plane angle mapping.

Snell's Law. Again, the transformation applies to a limited region around the optical center, where the distortion is relatively small. It may be emphasized that when mapping corresponding angles, it is assumed that the image exhibits only radial distortion.

Tsai[4,5] handled both extrinsic and intrinsic parameters in his calibration method. The extrinsic parameters are the rotation and translation matrices, while the intrinsic parameters are the effective focal length, one-pixel width on the image plane, optical center, and the distortion coefficients. Tsai's method is complicated and requires special techniques such as frequency measurement or 1-D FFT[5] for the calibration of one-pixel width. Error also arises in the case of high-distortion lenses.[4] Thus, a robust calibration procedure for high-distortion lenses has not been well established.[6]

Weng *et al.*[7] described several camera models, including radial, decentering, thin prism, and total distortion. Most commonly used methods discuss only the problem of radial distortion, but in our case a tangential component is introduced along with the radial distortion. This is theoretically known as decentering distortion. Actual optical systems are subject to various degrees of decentering, that is, the optical centers of the lenses are not strictly collinear with the CCD array. Here the pixel shift is away from the optical center and the new position lies at a new angle location as measured from the optical center. This kind of distortion can be analytically described by the following expressions:[8,9]

$$\delta_{pd} = 3(j_1\rho^2 + j_2\rho^4 + \cdots)sin(\psi - \psi') \quad (1)$$

$$\delta_{td} = (j_1\rho^2 + j_2\rho^4 + \cdots)cos(\psi - \psi') \quad (2)$$

where δ_{pd} is the radial distortion, δ_{td} is the tangential disortion, ρ is the distance to the pixel from the optical center, ψ is the angle between the pixel and the optical center, and $j_1, j_2, \ldots$ are the distortion coefficients. ψ' is the angle between the positive vertical axis and a line of reference which has the maximum tangential distortion.

The following section presents a method based on polynomial transformation for correcting the distortion in the images. The mapping is applicable to the complete image. Inverse mapping of the distortion coefficients is used to reconstruct the full gray scale undistorted image and the accuracy of the algorithm is then tested.

3. CAMERA CALIBRATION

This section presents the method for determining the optical center, the effective focal length, and one-pixel width on the image plane. It describes the calibration pattern used in the experiments and the method for correcting the barrel distortion.

3.1. *The optical center*

The optical center of any lens is defined as the point where the optical axis passing through the lens intersects the image plane of the CCD camera. The method we use is similar to Chang *et al.*[10] The optical center is found with the use of a low power laser beam. The setup is shown in Fig. 4. Initially, the iris of the camera is shut to avoid damage to the CCD. A low power laser beam is passed through a perforated white screen onto the center of the lens. The beam is partially reflected onto the white screen, forming a fringe pattern. The aim is to minimize the fringe pattern to a dot, thus ensuring that the beam is focused at the center of the lens. The pan and tilt of the laser beam, along with that of the lens, are adjusted until the laser beam reflects onto itslef. The goal is to align the laser beam and the optical axis of the lens. Once this is achieved, the laser beam is passed through an attenuating filter to lower the power of the laser beam to avoid damage to the CCD array. The iris is then opened slightly to capture a bright dot on the image plane. This dot indicates

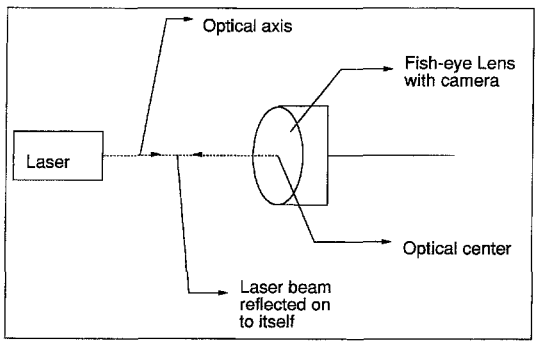

Fig. 4. Setup for optical center determination.

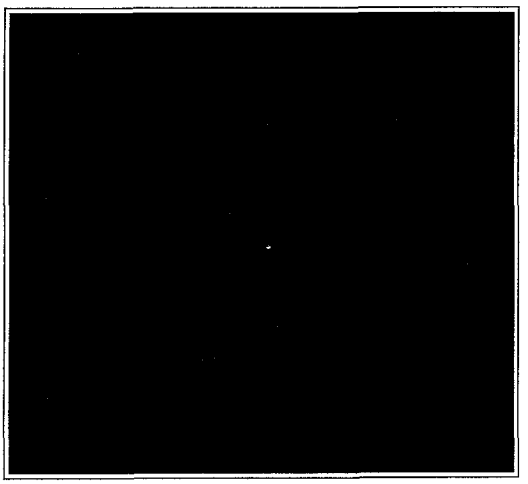

Fig. 5. The optical center.

the location of the optical center in the image plane. Figure 5 shows the image taken. The dot represents the optical center in the image plane. This method gives accurate and repeatable results.[10]

3.2. *The focal length*

We compute the focal length by assuming minimum distortion in the neighborhood of the optical center. This assumption is based on a pin-hole model camera. This implies that the points or pixels close to the optical center show negligible distortion or, ideally, no distortion. Thus, data points close tothe optical center have to be imaged. This is done by aligning the lens with its optical axis perpendicular to the calibration pattern. A mirror is placed on the calibration pattern and its live image is grabbed. Further, a cross-hair is displayed on the screen whose intersection is at the optical center of the lens. Using this view, the lens is aligned such that the lens sees itself in the mirror at the center of the cross-hairs. The cross-hair is to be aligned with its reflection and, as there is negligible distortion at the optical center, the horizontal and vertical lines of the cross-hair should intersect each other on the screen for points close to the optical center. The center dot in the calibration pattern image is also aligned in the center of the cross-hairs. This ensures that the center dot will not get distorted, nor will the dots in its immediate neighborhood. Once the lens is aligned, the distance D between the camera and the pattern is physically measured. L_y is defined as the distance between two points in the vertical direction lying close to the center of the pattern, and l_v is the distance in pixels between their perspective projections. The distances are represented by the schematic in Fig. 6. Assuming zero distortion near the center, the focal

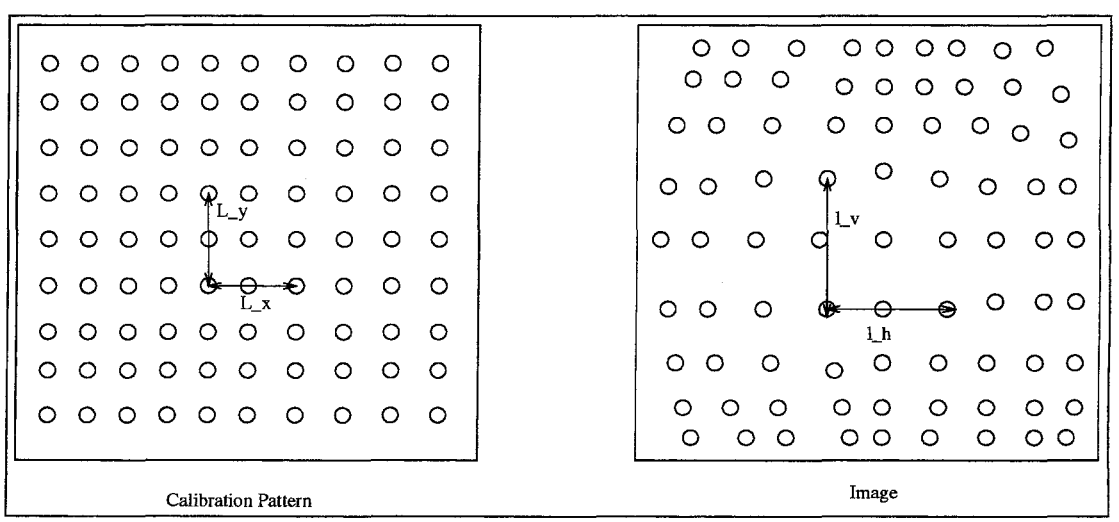

Fig. 6. Schematic showing the respective horizontal and vertical measures on the calibration pattern and the image.

Table 1. Determined one-pixel height and width

Pixel	Values (mm)
Width	0.017
Height	0.013

length is defined by

$$f = (l_v d_y) D / L_y \tag{3}$$

where d_y is the known one-pixel height on the image plane determined from the camera specifications.

One-pixel width on the image plane, d_x, cannot be determined from the camera specifications due to an imperfect match between the computer image acquisition hardware and the camera hardware. During scanning, spatially discrete signals picked up by each row of the sensor array are first converted to an analog waveform, which is then sampled by the computer image acquisition hardware into a number of spatially discrete samples and stored in a row of a image frame buffer. The number of sensor elements in a row of the sensor array and the number of picture elements in a row of the computer image frame buffer may not be same. In our case the buffer of the frame grabber is 512×484 while the size of the CCD array resolution is 510×492. Therefore, one must determine the one-pixel width on the image plane. The d_x is determined with the same lens setup used in focal length determination. This time, two horizontal data points close to the center are chosen as shown in Fig. 6. The one-pixel width in the image plane is then given by the relation

$$d_x = (L_x f)/(D l_h). \tag{4}$$

Here, L_x is the physical distance between the two horizontal points, f is the focal length computed earlier, and l_h is the horizontal distance in pixels as seen in the image plane. In our setup, $L_x = L_y$ as we use a pattern which has equally space dots. The values calculated for the one-pixel width and the given one-pixel height are shown in Table 1.

3.3. *The calibration pattern*

The calibration pattern consists of a grid of black dots placed every 10 cm, as shown in Fig. 1. The size of our pattern is 2.4×1.8 meters, which is about the size of the normal view seen by the lens. Each dot is used as a data point for image correction. As the calibration pattern is flat, and there is no variation in depth for any of the data points, it is easier to map its projections in the image plane. Further, by capturing just one image, sufficient data points are generated, so that repeated experimentation is avoided.

3.4. *Distortion correction procedure*

It is clear from the image acquired by the fish-eye lens that the lens exhibits distortion which may be represented in the polar domain. There is a transformation of angles along with relative distances. This is examined by taking data points from the calibration pattern and relating them to angles and pixel distances in the image plane to generate the distortion coefficients needed to correct the distortion. Since a combination of radial and tangential distortion is seen in the image, two sets of coefficients are needed to correct the distortion. If the distortion is symmetric in the four quadrants, then only one quadrant may be analysed. We use a polynomial transformation to correct the barrel distortion. A fifth order polynomial is used in this case to ensure the accuracy needed for precise calculations from the image. There is a trade off between the use of low order and high order polynomials. The former does not correct with the accuracy needed, while the latter makes the calculations computationally more expensive. The fifth order polynomial provides the best balance of accuracy and time taken for correction. We use two polynomials, one to correct the radius as measured from the optical center, and the

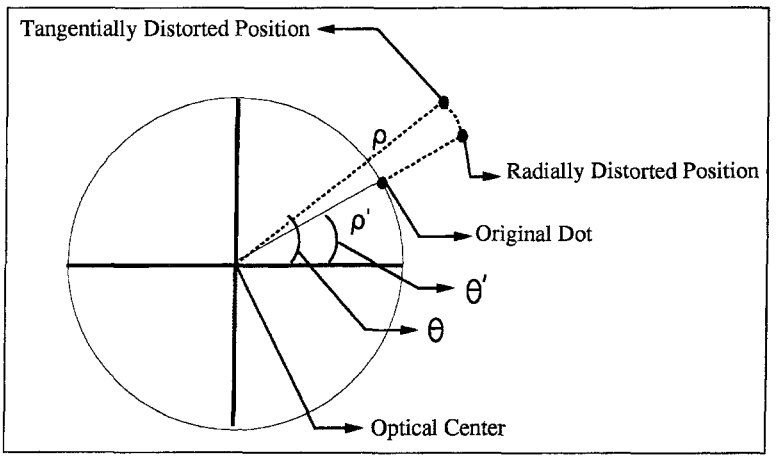

Fig. 7. The distortion model.

other to correct the polar angle as measured from the optical center. The polar angle is defined as the angle subtended by the line joining the projection of any point on the image plane and the optical center in the image plane. This angle is defined as θ, and θ' is the corrected angle. Similarly, ρ is the distance measured from the point projected in the image plane to the optical center, while ρ' is the corrected distance. The distortion model and the respective angles are shown in Fig. 7. Thus, we simultaneously correct the radial position of each pixel and at the same time correct the tangential offset component. The general equations used are:

$$\theta' = a\theta + b\theta^2 + c\theta^3 + d\theta^4 + e\theta^5 \tag{5}$$

$$\rho' = f\rho + g\rho^2 + h\rho^3 + i\rho^4 + j\rho^5 \tag{6}$$

where θ' is the corrected angle, θ is the angle as imaged by the fish-eye lens, ρ' is the corrected radius, ρ is the radius as viewed by the fish-eye lens, and a through j are the distortion coefficients. In the above equation, we do not have a constant term, as the distortion at the optical center is zero. From the calibration pattern, the actual position of each dot is computed based on the pixel width and the pixel height. The location of each distorted black dot is also calculated from the image. In this manner, the distortion data is generated, and using a repeated Lagrangian minimization procedure, the distortion coefficients are estimated. These coefficients are further optimized by using *a priori* knowledge. Imaging three data points in a straight line should result in them being in a straight line in the image plane. The difference in the slopes of lines passing through the first two and the last two data points is minimized until it reaches zero, thus optimizing the accuracy of the transformation polynomial. This step ensures that the polynomial coefficients that are determined are not an overfit to the data. This method also compensates for any accuracy errors that might be present while determining the image point correspondences to their respective locations on the calibration pattern. Finally, the technique of inverse mapping is used to recover the complete gray-level image.

3.4.1. *Lagrange minimization.* Having established the point correspondences in the original pattern and the distorted pattern, we have a data set which indicates a certain transformation. To represent this transformation with an optimal polynomial and determine the distortion coefficients, the method of Lagrange minimization is used. For our data points, there is only one polynomial of the fifth order that passes through all the points. This polynomial is approximated by the function:

$$F_n(x) = \sum_{r=0}^{n} Y_r(x) f(x_r) \tag{7}$$

where Y_r is the Lagrange formulation term, $f(x_r)$ is the data point at r, and $F_n(x)$ is the coefficient of the polynomial. The Lagrange formulation term is given by:

$$Y_r(x) = \prod_{s \neq r, s=0}^{n} \frac{x - x_s}{x_r - x_s}. \tag{8}$$

The above formulation can be generalized to determine the polynomial of the required order. For the case of a second-order polynomial the formulation can be expressed as:

$$F_2(x) = \frac{(x - x_1)(x - x_2)}{(x_0 - x_1)(x_0 - x_2)} f(x_0) + \frac{(x - x_0)(x - x_2)}{(x_1 - x_0)(x_1 - x_2)} f(x_1) + \frac{(x - x_0)(x - x_1)}{(x_2 - x_0)(x_2 - x_1)} f(x_2) \tag{9}$$

where x_r and $f(x_r)$ are the points in the data set representing the transformation.

3.4.2. *Inverse mapping.* The distortion coefficients determined above form a transform from the distorted image to the corrected image which represents a one-to-one mapping. The mapping so established forms a new image which is four times the size of the original image. As there are fewer points to map, we see the presence of blank spots in the corrected image. It is essential to recover the complete gray-scale image to do any further processing based on intensity values. To achieve this objective, we use the technique of inverse mapping, which forms a mapping of points corresponding to the new locations of the pixels in the undistorted image. The distortion correction coefficients are then determined by considering the pixel locations in the undistorted image and its corresponding mapping in the distorted image. Thus a new transform relationship between the undistorted and the distorted image is established which has a many-to-one relationship. This results in the mapping of one or more pixels in the undistorted image to a single pixel in the distorted image. The coefficients so determined are the inverse coefficients of the transform and are able to reconstruct the complete gray-level intensity of the corrected image.

3.5. *Coordinate system*

In order to accurately determine the location of any point in 3-D space, it is important that we know the precise location of the camera and its viewing geometry. To better understand the transformation of points from the 3-D space to their corresponding position in the image plane, we briefly discuss the camera coordinate system.

The camera and the world coordinate system used are shown in Fig. 8. **W** represents the world coordinate system with a vertical z-axis, **M** the camera mount coordinate system, **C** the camera coordinate system, and **P** the image coordinate system (used for the perspective projection on the CCD of the camera). Let

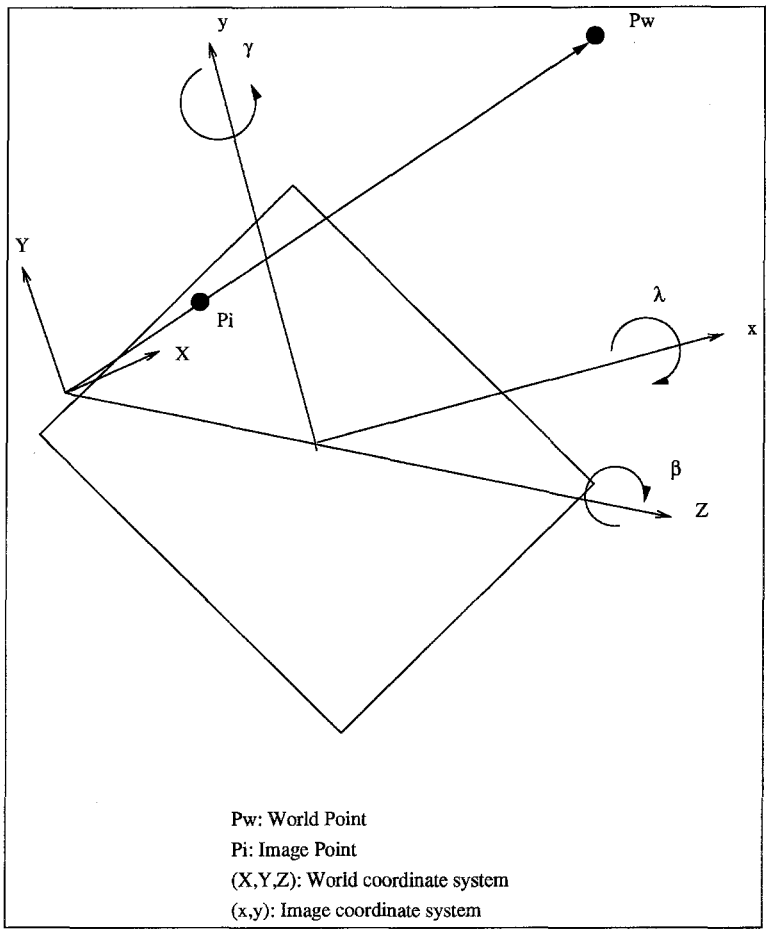

Fig. 8. Camera coordinate geometry.

h, r and p represent the heading, roll and pitch of the camera mount. The transformation from **W** to **C** is given by:

$$T_{WC} = T_{WM} T_{MC}. \tag{10}$$

T_{WM}, the homogeneous coordinate transformation matrix from **W** to **M** is given by:

$$T_{WM} = T_r \cdot \begin{bmatrix} 1 & 0 & 0 & 0 \\ 0 & \cos p & \sin p & 0 \\ 0 & -\sin p & \cos p & 0 \\ 0 & 0 & 0 & 1 \end{bmatrix} \cdot \begin{bmatrix} \cos h & \sin h & 0 & 0 \\ -\sin h & \cos h & 0 & 0 \\ 0 & 0 & 1 & 0 \\ 0 & 0 & 0 & 1 \end{bmatrix} \cdot \begin{bmatrix} 1 & 0 & 0 & -x \\ 0 & 1 & 0 & -y \\ 0 & 0 & 1 & -z \\ 0 & 0 & 0 & 1 \end{bmatrix}, \tag{11}$$

where T_r represents the transformation matrix associated with the roll of the camera mount, p and h represent the pitch and heading of the camera mount, and x, y and z represent the relative position of the camera mount with respect to the world. T_{MC}, the coordinate transformation matrix from **M** to **C**, is completely determined through eye-mount calibration which is similar to the procedure detailed in references (10, 11). Finally, the perspective projection from camera to image plane is given by:

$$\begin{bmatrix} su \\ sv \\ s \\ 1_p \end{bmatrix} = \begin{bmatrix} \alpha_u f & u_0 & 0 & 0 \\ 0 & v_0 & -\alpha_v f & 0 \\ 0 & 1 & 0 & 0 \\ 0 & 0 & 0 & 1 \end{bmatrix} \begin{bmatrix} x \\ y \\ z \\ 1_c \end{bmatrix} \tag{12}$$

where u and v represent the coordinates of a point on the image plane (pixels) α_u and α_v are conversion factors (pixels per unit length), u_0 and v_0 are the coordinates of the optical center of the camera (pixels), and f is the focal length (unit length). These parameters are determined through the calibration of the camera as described above. s represents the depth, and therefore cannot be determined from a single image.

4. RESULTS

The fish-eye lens used in the experiments is manufactured by Toyo Optics and has an effective calculated focal length of 3.8 mm. The horizontal field of view of

Fig. 9. Corridor as imaged by the fish-eye lens.

the lens is $\sim 138°$ and the diagonal field of view is $\sim 178°$. The lens is mounted on a Panasonic solid-state CCD camera with 510×492 image sensing elements. The CCD has a scanning area of $6.6 \times 8.8\ \text{mm}^2$ and the image buffer used is 512×484 pixels.

Figure 9 shows a 512×480 image of a corridor taken with the fish-eye lens. One can see the bending of various structures due to excessive barrel distortion. This image was corrected using the polynomial transformation. The corrected image is as seen in Fig. 10. Each pixel in the distorted image is corrected and mapped to the new image. When corrected, the image generated is more than four times the size of the original image. In Fig. 10, the size is restricted to 1024×960 pixels. As shown, many blank pixels have been introduced into the corrected image. This is due to the fact that the original image has only 512×480 pixels to be mapped on to the new, larger image. We can also see blank areas in the horizontal and the vertical image ends due to the larger field of view in the diagonal direction than any other direction.

The problem of blank pixels is solved by using inverse mapping, as discussed earlier. A mapping relating the pixel location in the final corrected image to the pixel location in the distorted image is used to determine the coefficients of the polynomial. The distortion coefficients are then applied to find a pixel location in the original image from the pixel location in the final corrected image. Thus it is possible that several pixels in the final image may map to the same pixel in the original image. In this way, all the pixels in the new image are mapped, thus generating a complete, undistorted image. Even with this mapping, the blank areas at the horizontal and vertical ends cannot be eliminated. To remove blank area we limit the size of the new image to that of the old image. As seen in Fig. 11, little information is lost, and the problem of barrel distortion is resolved. The distortion coefficients used for

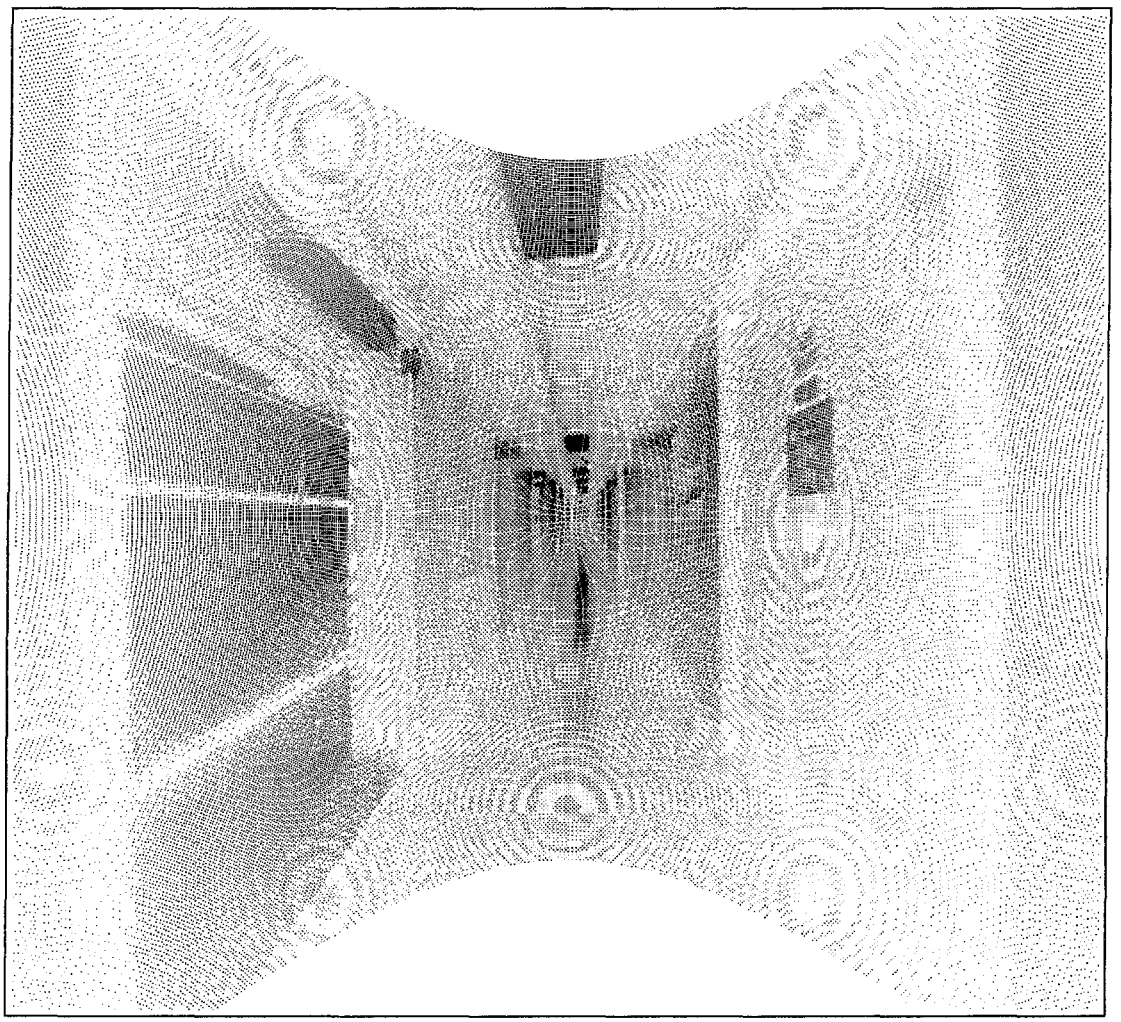

Fig. 10. Corrected image of corridor (1024 by 960).

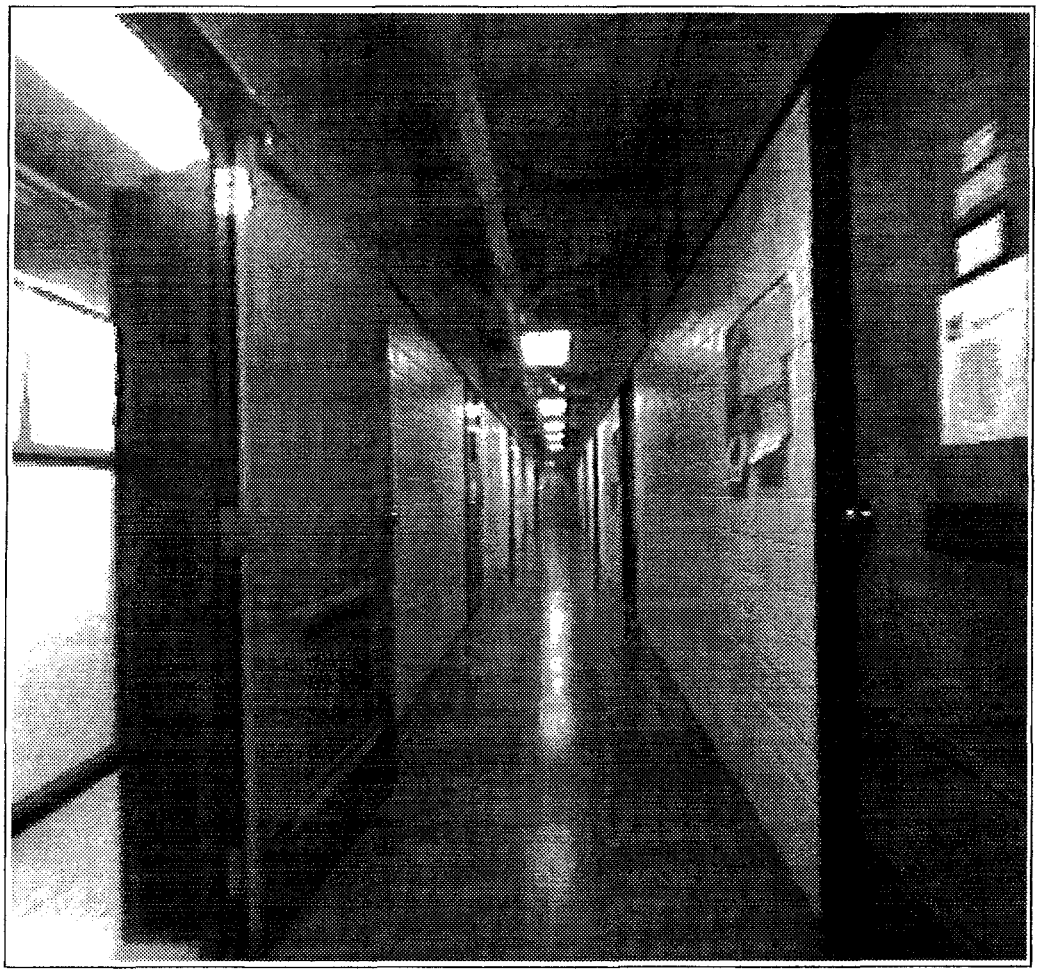

Fig. 11. Corrected image using inverse mapping.

Table 2. Radial distortion coefficients used for image correction

	Coefficients				
Distortion	a	b	c	d	e
Radial	0.81035	−6.2546e-2	0.26003	−0.12455	2.1225e-2

Table 3. Tangential distortion coefficients used for image correction

	Coefficients				
Distortion	f	g	h	i	j
Tangential	1.14190	−0.74194	0.53545	−0.15083	1.17113e-2

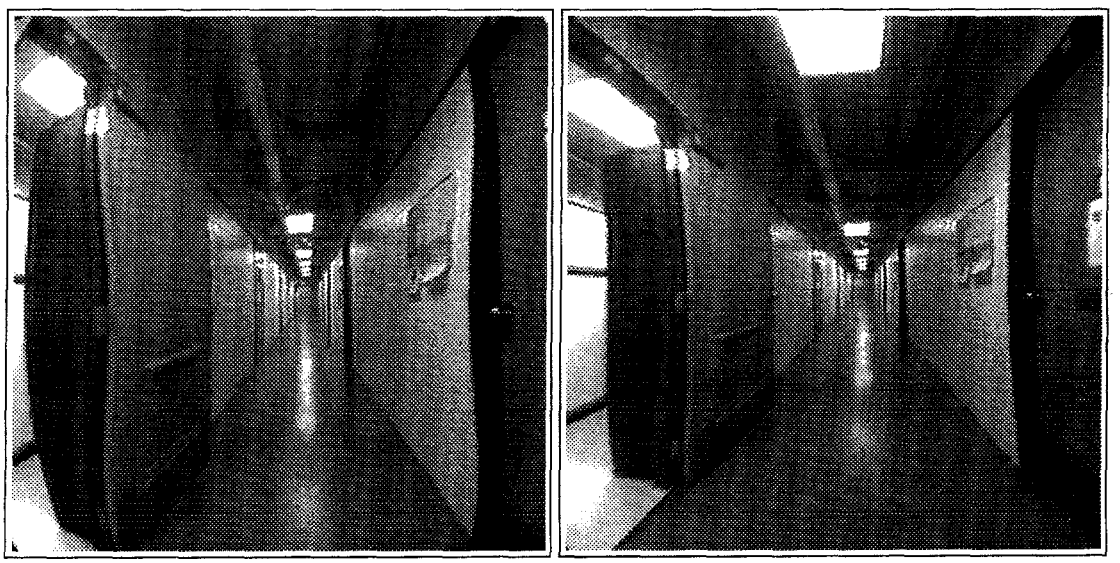

Fig. 12. Corrected image of corridor using a 5th order (left) and 7th order (right) odd powered polynomial.

image correction are given in Tables 2 and 3. Coefficients a to e are used for correction of radial distortion, while the coefficients f to j are used for tangential distortion correction.

In order to determine the symmetry of the distortion, we consider a polynomial of odd powers. Such a polynomial would result if the distortion exhibited is radially symmetric. Once again a Lagrangian minimization is performed to determine the coefficients of the odd powered polynomial, and even powers are set to zero. We consider both a fifth order polynomial and a seventh order polynomial. The corrected image using a fifth order and seventh order odd powered polynomial is seen in Fig. 12. The images still exhibit distortion and the correction is not adequate. This shows that the distortion seen, known as barrel distortion, is not entirely radially symmetric and exhibits a combination of distortions.

The algorithm is implemented on a HP 735 workstation and the image correction takes approximately 4 s.

5. ACCURACY

To test the accuracy of the corrected image, a series of images was taken at 1 meter intervals (Fig. 13) and the line segments were detected (Fig. 14). Actual lengths of the edges in the horizontal and vertical direction were measured in the real world, and their distances from the lens were recorded. All segments which did not have known end points were neglected. Next, each segment in the image plane was measured.

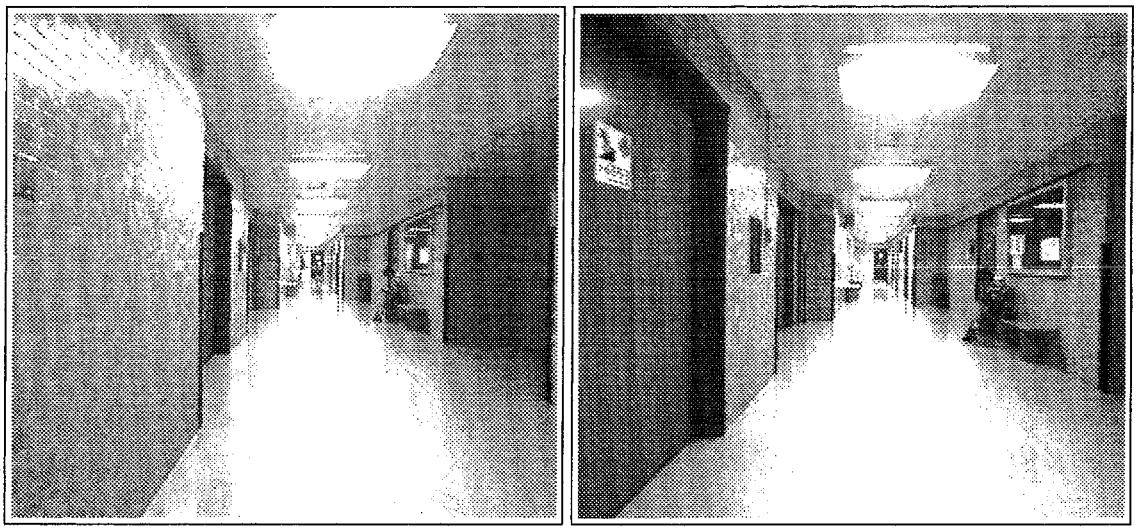

Fig. 13. Images taken at 1 meter interval.

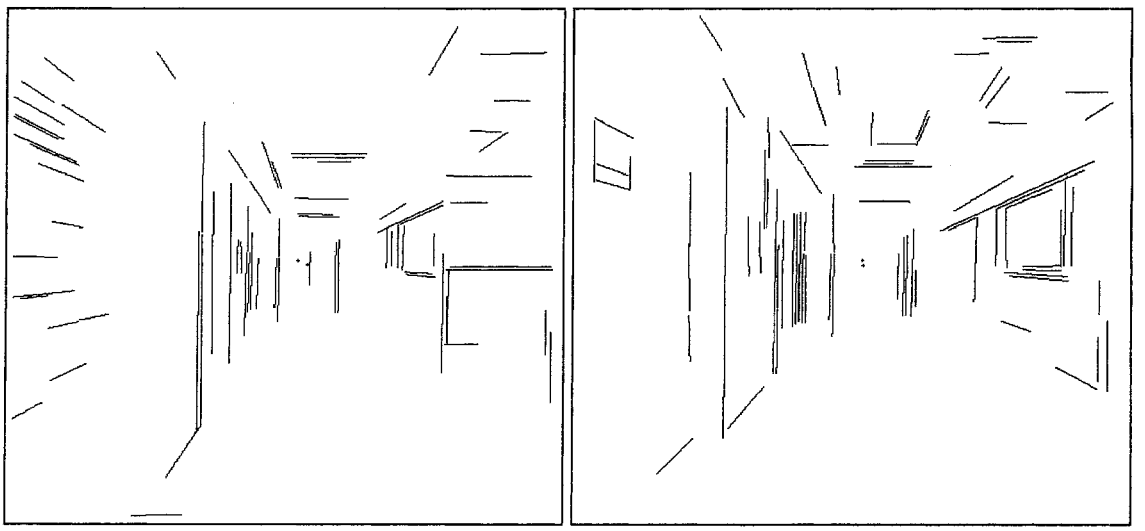

Fig. 14. Line detected images.

Their length was computed using the equation:

$$l_x = (fL_x)/(Zd_x) \tag{13}$$

or

$$l_y = (fL_y)/(Zd_y) \tag{14}$$

where f is the effective focal length of the lens, L_x and L_y is the horizontal and vertical length respectively, of the edge in the real world, Z is the distance of the edge from the lens in the real world, and d_x is the pixel width, in the case of a vertical edge, and d_y is the pixel height, in the case of a horizontal edge. The computed lengths were compared to the actual measured lengths in the real world and an accuracy of within 2% was established, with the maximum error occuring towards the edge of the image. Table 4 shows the distribution of detected segments and the average error in length calculation.

Table 4. Length error distribution

Detected line classification				
		Average length distribution (mm)		
Segments	#	Length	Det. length	Error
Vertical	23	1473.2	1449.8	1.6%
Horizontal	17	515.96	509.7	1.4%
Total	40	1990.16	1959.5	1.54%

6. CONCLUSION

In this paper, we have presented a simple but effective procedure for the calibration of a high distortion lens. The determination of intrinsic parameters using a simple calibration procedure is addressed. The parameters calibrated include the distortion coefficients, the optical center, the effective focal length, and the one pixel width on the image plane. A camera model for fish-eye lenses is presented and the distortion characteristics are analysed. In the calibration procedure, the polynomial transformation is calculated for a camera which has two components of distortion, radial and tangential. The polynomial is calculated using Lagrange minimization and the coefficients are further optimized using *a priori* information. The technique of inverse mapping is used to account for the blank areas in the undistorted image and to recover a complete gray-level image. The calibration procedure is successfully applied to real world images acquired using the fish-eye lens, and the accuracy of the correction is established.

REFERENCES

1. C. Beck, Apparatus to photograph the whole sky. *J. Sci. Instrument.* **2**, 135–139 (1925).
2. K. Miyamoto, Fish eye lens. *J. Lett.* **54**, 1060–1061 (1964).
3. R. L. Anderson, N. Alvertos and E. L. Hall, Omnidirectional real time imaging using digital restoration, *SPIE High Speed Photograph*, **348** (1982).
4. R. Y. Tsai, A versatile camera calibration technique for high accuracy 3D machine vision metrology using off the shelf TV cameras and lenses. *IEEE J. Robotics Automat.* **3**, 323–344 (August 1987).
5. R. K. Lenz and R. Y. Tsai, Techniques for calibration of the scale factor and image center for high accuracy 3-D machine vision metrology, *IEEE Trans. Pattern Anal. Mach. Intell.* **10**, 713–720 (September 1988).
6. Y. Nomura, M. Sagara, H. Naruse and A. Ide, Simple calibration algorithm for high-distortion-lens camera, *IEEE Trans. Pattern Anal. Mach. Intell.* **14**, 1095–1100 (November 1992).
7. J. Weng, P. Cohen and M. Herniou, Camera calibration with distortion models and accuracy evaluation, *IEEE Trans. Pattern Anal. Mach. Intell.* **14**, 965–981 (October 1992).
8. D. C. Brown, Decentering distortion of lenses, *Photogrammetric Eng. Remote Sensing*, 444–462 (May 1966).
8. *Manual of Photogrammetry*. 4th edn., Amer. Soc. Photogrammetry (1980).
10. Y. L. Chang, X, Lebegue and J. K. Aggarwal, Calibrating a mobile camera's parameters, *Pattern Recognition*, **26**, 75–88 (1993).
11. X. Lebègue and J. K. Aggarwal, A mobile robot for visual measurements in architectural applications, *Proc. IAPR Workshop on Mach. Vis. Appli.* 195–198, Tokyo, Japan (December 1992).

About the Author—J. K. AGGARWAL has served on the faculty of The University of Texas at Austin College of Engineering since 1964 and is currently the Cullen Professor of Electrical and Computer Engineering and Director of the Computer and Vision Research Center. His research fields include computer vision, parallel processing of images, and pattern recognition. He has been a Fellow of IEEE since 1976. In 1992, he received the Senior Research Award of the American Society of Engineering Education. Dr Aggarwal is author or editor of seven books and 31 book chapters; author of over 160 journal papers, as well as numerous proceedings papers, and technical reports. He has served as Chairman of the IEEE Computer Society Technical Committee on Pattern Analysis and Machine Intelligence (1987–1989); Director of the NATO Advanced Research Workshop on Multisensor Fusion for Computer Vision, Grenoble, France (1989); and Chairman of the IEEE Computer Society Conference on Computer Vision and Pattern Recognition (1993). He currently serves as IEEE Computer Society representative to the International Association for Pattern Recognition, is Past President of the International Association for Pattern Recognition, and is an Editor of IEEE *Transactions on Parallel and Distributed Systems.*

About the Author—SHISHIR SHAH received the B.S. degree in mechanical engineering in 1994, and the M.S. degree in electrical engineering in 1995 from The University of Texas at Austin. He is presently working toward the Ph.D degree at the Computer and Vision Research Center, The University of Texas at Austin. His research interests include mobile robots, computer vision, and pattern recognition. Mr Shah is a student member of the IEEE Computer Society.